Electrolysis of rich Titanium Slag in Molten CaCl₂ with a Liquid Zn Cathode

*Wei Dai[1], Bo Qin[1,2] ***, *Yingxin Liu[1], Hengwei Yan[1,2], Wenhui Ma[1]*

[1] Faculty of Metallurgical and Energy Engineering, Kunming University of Science and Technology, Kunming 650093, China
[2] State Key Laboratory of Complex Nonferrous Metal Resources Clean Utilization, Kunming University of Science and Technology, Kunming 650093, China
*E-mail: 59077730@qq.com

A unique utilizing method for rich titanium slag with liquid Zn cathode in molten CaCl₂ has been proposed. In order to establish this process, the electrochemical behavior of TiO₂ was investigated. Cyclic voltammetry results showed that the reduction of TiO₂ on Zn electrode at 1123 K was occurred at potential range from -0.77 V to -1.73 V vs. Ag/AgCl. After potentiostatic electrolysis at -1.5 V, reduction and enrichment of Ti in Zn matrix was confirmed by EDS, XPS and XRD. The content of titanium reached 26.3 at% in the rich region. The electrolysis of rich titanium slag with Zn electrode was carried out. Metal Ti can be observed in Zn matrix after electrolysis only after a pre-melting process was carried out. The content of Ti in the enriched area was increased from 5.5 at% to 25.4 at% when the pre-melting time increased from 1 hour to 3 hours.

1. INTRODUCTION

It is well known that titanium is an important element which occurs in nature primarily as the oxide. Titanium is widely used in many fields because of its unique corrosion resistance, heat resistance, strength superiority and good biocompatibility [1,2]. There are two principal ores including rutile and ilmenite. Ilmenite is a mixture of titanium and iron oxides. Smelting of the ilmenite is the most common process to prepare rich titanium slag (Ti-slag) and produce pig iron by carbothermal reduction. Nowadays, to produce titanium pigment by chlorination is the development tendency of the worldwide titanium pigment industry, but the chloride process needs a high grade of Ti-slag. However, the contents of CaO and MgO in ilmenite in China is higher than that in other countries, which is not suitable for

production of Ti-slag because of high content of calcium and magnesium. Therefore, it is necessary to look for a way to utilize and process ilmenites which have high content of impurities.

The Kroll process is the dominant technology for the production of titanium metal in industrial process [3-6]. Due to high energy consumption and discontinuity of production Ti in Kroll process, which leads to high cost of titanium further limits the application of titanium and its alloys. The electrochemical deoxidation technologies can be used to extract titanium metal from solid titanium dioxide in molten salts since FFC Cambridge process was reported in 2000 [7]. The FFC process, which had the potential for replacement Kroll process to achieve low-cost production of titanium metal, received considerable attention. This method can also be applicable to the preparation of other metals and alloys by solid metal oxide molten salt electrolysis [8-13].

However, dense TiO_2 pellet is used as cathode after compacted and sintered which caused long electrolysis time and low current efficiency [14,15]. In order to avoid these problems, some papers were reported that the advantages of using liquid metal cathode in molten salt electrolysis are less process, low energy consumption and easy separation [16-21]. In this work, electrolysis of rich titanium slag was studied in molten $CaCl_2$ with a liquid Zn cathode. The behavior of TiO_2 on liquid Zn electrode was also investigated by cyclic voltammetry.

2. EXPERIMENTAL

2.1 Cathode assembly and electrochemical test
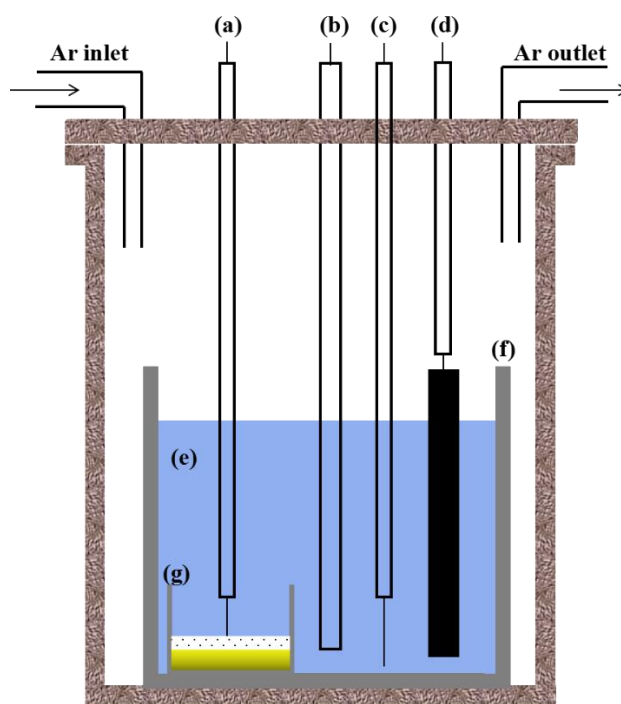
Figure 1. Schematic illustration of electrolysis apparatus. (a) TiO_2/Zn cathode (b) Ag/AgCl reference electrode (c) Mo electrode for pre-electrolysis (d) graphite counter electrode (e) $CaCl_2$ (f) the bigger Al_2O_3 crucible (g) the smaller Al_2O_3 crucible

Zn granules (analytical grade, 3-5mm, 2.5g) were placed at the bottom of a corundum (inner diameter 11mm, outer diameter 13mm, height 21mm). The TiO_2 powder (analytical grade, 2-3um, 0.3g) laid on the part of the metal. Calcium chloride was selected as the electrolyte. According to the Ti-Zn binary phase diagram, the solubility of titanium in Zn is about 6.5 at% at 1123 K, although the vapor pressure of Zn is large, the volatilization of Zn can be greatly suppressed by the $CaCl_2$ melt [19]. The densities of liquid Zn, solid TiO_2 powder and molten $CaCl_2$ are $5.9g \cdot cm^{-3}$, $4.23g \cdot cm^{-3}$, $2.2g \cdot cm^{-3}$, respectively. In order to ensure that the TiO_2 powder and the Zn particles can form a distinct three phases interface $CaCl_2/TiO_2/Zn$ in the crucible at the experimental temperature, the mass ratio of TiO_2 to Zn is less than 15:100. A Mo wire (diameter 3mm, 99.9%) threaded into an alumina insulating tube (inner diameter 4mm, outer diameter 6mm, 99.9%) was used as current lead inserted the Zn layer and formed a TiO_2/Zn compound electrode. Solid TiO_2 powder was placed on the top of the Zn particles. When the temperature rises, the metal evolves from solid to liquid and forms the compound electrode together with TiO_2 powder. Electrons are supplied from the Mo wire to the liquid metal. If titanium is reduced, it will alloy with zinc at the bottom. $CaCl_2$ (analytical grade,1-2mm, 140g) was charged in a bigger corundum (inner diameter 52mm, outer diameter 60mm, height 120mm) which contained the Zn/TiO_2 compound electrode. The bigger corundum was placed in a vertical resistance furnace with sealed quartz cell to remove moisture maintaining at 573 K for 12 h and then melt at 1123 K for 3 h (the process which temperature was higher than the melting point of $CaCl_2$ and melted for minutes named as pre-melting) under dried argon atmosphere. Pre-electrolysis was carried out at 1.6-2.8 V to remove residual moisture and oxide ions from the molten salt. Pre-electrolysis and all electrochemical experiments were performed in a dried argon atmosphere (260-300 $ml \cdot min^{-1}$) at 1123 K. Cyclic voltammetry (CV) was performed by a Zahner electrochemical workstation controlled with Thales 3.04 software. Figure 1 shows the scheme of the electrochemical apparatus for electrochemical examination. A spectral pure graphite rod (diameter 6mm, height 80mm) connected a Mo rod with alumina insulating tube was used as anode. The reference electrode was Ag/AgCl couple, which consisted of a silver wire (diameter 1mm) encased in a mullite tube in AgCl (0.5mol%)-$CaCl_2$ mixture. Electrochemical behavior of molten salt, liquid Zn electrode, TiO_2/Zn compound electrode was measured respectively by cyclic voltammetry.

2.2 Electrolysis of TiO_2 and rich titanium slag with a liquid Zn electrode.

Table 1. Chemical composition of high titanium slag from some plant of China (mass fraction %)

Component	TiO_2	Fe_2O_3	SiO_2	MgO	Al_2O_3	CaO
Concentration	70.33	9.96	7.12	6.21	2.96	1.5

Pre-melting and pre-electrolysis were completed, the potentiostatic electrolysis was directly performed on Zn/TiO_2 compound electrode or high titanium slag on the liquid Zn electrode. TiO_2 or rich titanium slag with Zn electrode was used as the cathode, graphite rod was used as the anode. The

chemical composition of rich titanium slag obtained from some plant of China was analyzed by X-ray fluorescence spectrometer (XRF) and shows in table 1.

Rich titanium slag was ground in a ball mill for more than 30 minutes to obtain sufficient particle size before electrode assembled. Meanwhile, the mass ratio was the same as the TiO$_2$/Zn electrode. The sample obtained from cathode was cooled to room temperature and washed by water after electrolysis. The product was cut into 3 parts. The middle part was taken to polish with abrasive paper and to buff even surface smoothed. The microstructure and element distribution in Zn matrix after electrolysis can be detected by back-scattered scanning electron microscopy (SEM) equipped with an energy dispersive spectrometer (EDS). The valance of Ti and Zn was analyzed by the X-ray photoelectron spectroscopy (XPS). The X-ray diffraction (XRD) was used to observe the phases.

3. RESULTS AND DISCUSSION

3.1 Cyclic voltammetry
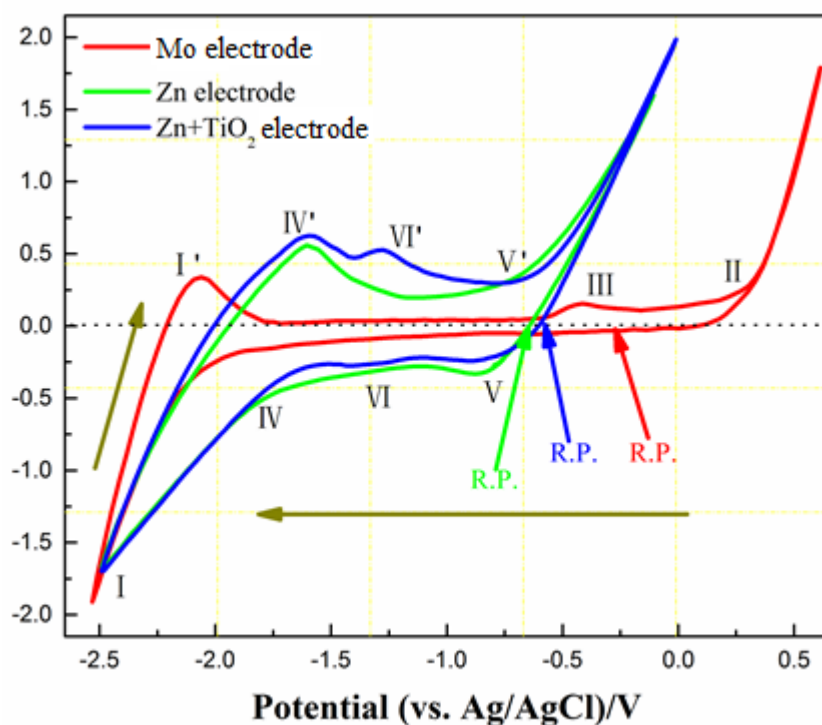
Figure 2. Cyclic voltommetry curves of Mo electrode (red), Zn electrode (green) and Zn/TiO$_2$ electrode (blue) in molten CaCl$_2$ with a scan rate of 100 mV/s at 850°C. The potential is swept in the cathodic direction from the open circuit potential.

Figure 2 shows the cyclic voltammograms of Mo electrode (red color), Zn electrode (green color) and TiO$_2$/Zn compound electrode (blue color). The possible reactions are shown in table 2. Mo wire was used as the working electrode to investigate the electrochemical behavior of calcium chloride. The main electroactive substance in the molten salt was the oxidation of Cl$^-$/Cl$_2$ as reaction (2) and showed an abrupt increase in anode current near 0.21 V (vs. Ag/AgCl) in the positive scanned. Due to the reduction

of metallic calcium as the reaction (1) in the negative direction, the cathode current showed a rapid increase near -1.91 V (vs. Ag/AgCl). Likewise, there was a corresponding dissolution of calcium around -2.1 V. Before the evolution of chlorine gas, there was a mild peak, and the anode current showed a gentle increase at -0.41 V (vs. Ag/AgCl).

Table 2. The reactions and corresponding potentials in cyclic voltammograms

Number	Reaction	Potential/ V (vs. Ag/AgCl)
1	$Ca^{2+}+2e^-\rightarrow Ca(l)$	-1.91 V
2	$2Cl^-\rightarrow Cl_2(g)+2e^-$	0.21 V
3	$O^{2-}+C\rightarrow COx(g)+2e^-$	-0.41 V
4	$Ca^{2+}+2e^-+Zn(l)\rightarrow Ca+Zn(l)$	-1.73 V
5	$Zn^{2+}+2e^-\rightarrow Zn(l)$	-0.77 V
6	$TiO_n+2ne^- \rightarrow Ti+nO^{2-}(n\leq2)$	-0.77~ -1.73 V

It was believed that before the releasing of chlorine gas (potential difference 0.7 V), the oxidation of residual O^{2-} in the molten salt formed CO_x gas as the reaction (3), which resulted in a relatively gentle increasing in anode current [22]. The released O^{2-} was diffused to the anode under the action of current, where the same process occurred again necessarily transferring C from anode to cathode, which leads to the pollution of carbon and the increasing energy consumption [23]. It is considered that the appearance of the impurity peak in the $CaCl_2$ cyclic voltammogram is caused by the CO_x gas evolution as reaction (3) and the corresponding reduction reaction showed as following.

$$CO_2+4e^-\rightarrow C+O^{2-} \tag{1}$$

Mo wire inserted into the corundum with Zn as the working electrode to investigate the electrochemical behavior of Zn electrode (green color). It was found that there is an obvious cathode current in the negative direction near about -1.73 V (vs. Ag/AgCl). After potentiostatic electrolysis at -1.8 V for 30 min, the electrolysis product was detected by the EDS. The sample was Ca-Zn alloy, where the content of calcium was about 4.59-4.73wt%. The reaction (4) at -1.73 V (vs. Ag/AgCl) was the reduction of calcium ion on Zn electrode, which is more positive than the result obtained by the molybdenum wire electrode. The difference is caused by the depolarization of the liquid Zn electrode. In general, when the product is soluble in the electrode surface, the actual potential becomes smaller than the standard electrode potential.

In addition to the deposition and resolution of calcium, the anode current showed a rapid increase at -0.77V (vs. Ag/AgCl), which is possibly caused by the dissolution of Zn. It is reported in the literature [19] that the addition of $CaCl_2$ can largely inhibit the volatilization of Zn. The concentration of Zn in molten $CaCl_2$ only 0.94wt% after smelt at 1123 K for 24 h. In fact, after pre-electrolysis for 3h, a small amount of Ca-Zn alloy was precipitated at the bottom of the crucible. Therefore, the increase of the anode current at -0.77V is caused by the dissolution of Zn, there was a reduction peak in the negative

scanning region. This is attributed to the formation of liquid Ca–Zn alloy because Ca and Zn form a liquid phase over the entire composition range at 1123 K. Calcium is soluble to 3.7 mol % at 900°C [24], which is beneficial for calcium reduction due to the solubility of the metals increasing in their own chlorides. Molten calcium chloride is a preferred electrolyte for molten salt process because of its stability and high oxide anion solubility [25]. The oxygen ionization process is a primary reduction reaction for the metal reduction in molten salt. The process of calcium reduction is considered as a secondary reaction. The calcium cations were reduced to calcium, and then the metal was deposited on the cathode surface.

TiO_2/Zn compound electrode used as the working electrode to investigate the electrochemical behavior of TiO_2 on Zn electrode (blue color). After adding TiO_2 powder to the liquid Zn electrode, there was another obvious peak in the anode current during the positive scanning. The corresponding reduction peak existed between the deposited current of Ca and Zn. It was occurred the reduction of TiO_2 on Zn electrode in the potential range from -0.77 V to -1.73 V (vs. Ag/AgCl) as the reaction (6). The open circuit voltage was -0.59 V, which is more positive than that of Zn electrode (-0.65 V). TiO_2 powder can't be reduced by liquid Zn according to thermodynamic calculation. The reduction of titanium oxide was the main cathodic reaction. The main controlled process is electron transfer towards the process of electro-deoxidation of TiO_2.

3.2 TiO₂ /Zn compound electrode electrolysis

On the basis of the cyclic voltammetry results, the potentiostatic electrolysis conducted at -1.5 V for 2 h. Fig 3(a) shows the current-time curves. The current dropped to 60 mA in 18 minutes, and then it had almost no change. The photographs of production from cathode became gray black when it was placed in air for three weeks after cut. Fig 3(b) shows the sample after polished and buffed. The images of SEM with EDS point scan illustrate as Fig 3(c) and (d). There was a heart-shaped dark area (20 um in length) to exist in the Zn matrix. In the dark region, it included Zn, Ti, Al, where the content of Ti and Al reached 26.3 at%, 15 at% respectively. It agrees with the results that Ti was reduced between the deposition of Ca and Zn. The content of Ti is significantly improved than the electrolysis of TiO_2 pellets with Bi electrode which has a larger solubility of Ti [16]. Al might be from the reduction of Al_2O_3 crucible. Other areas were almost pure zinc metal. Rang from 0 to 0.8 of the band, there were very small C and O peaks, where the total content was less than 1 at%. For the purpose of the study the reduction process of TiO_2 on Zn electrode, valance of Ti and Zn in the product was analyzed by XPS. As represented in fig 3 (e) and (f), the appearance of zero-valance titanium (454.2 eV) in Zn could prove the reduction of titanium. However, in addition to zero valance Ti and Zn, tetravalent and bivalent titanium and bivalent zinc were detected. XRD was advanced as shown in fig 4.
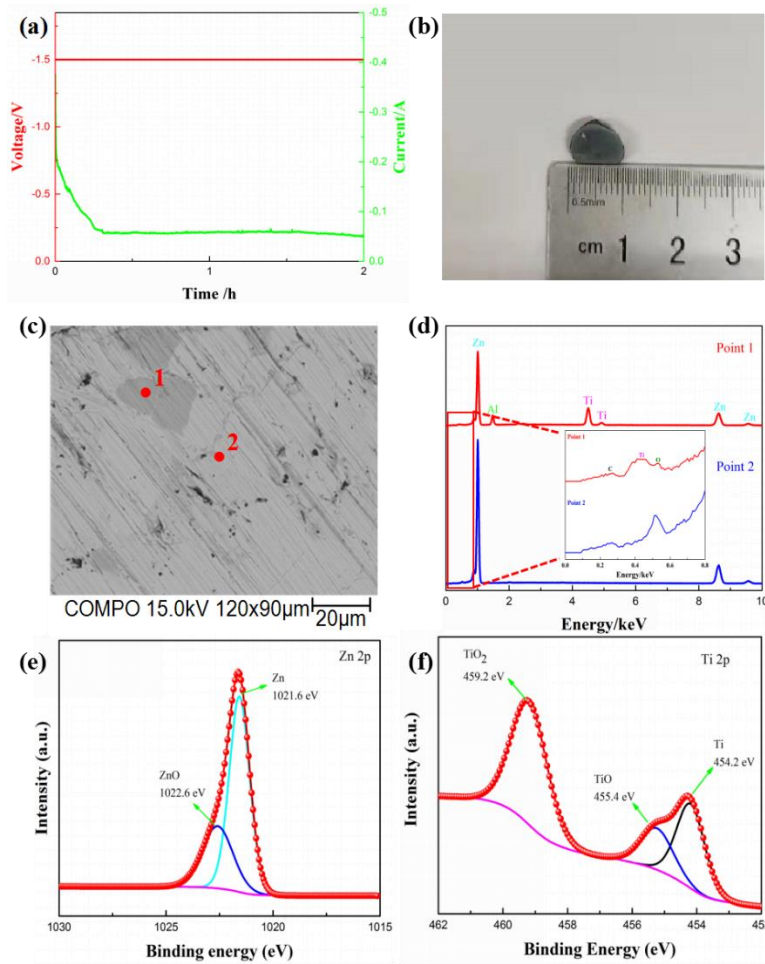
Figure 3. (a) Current-time curves (b) Photographs of production (c) SEM (d) EDS point scan (e) XPS image of Ti 2p spectrum (f) XPS image of Zn 2p spectrum of Zn/TiO_2 electrode after potentiostatic electrolysis at -1.5 V for 2 h
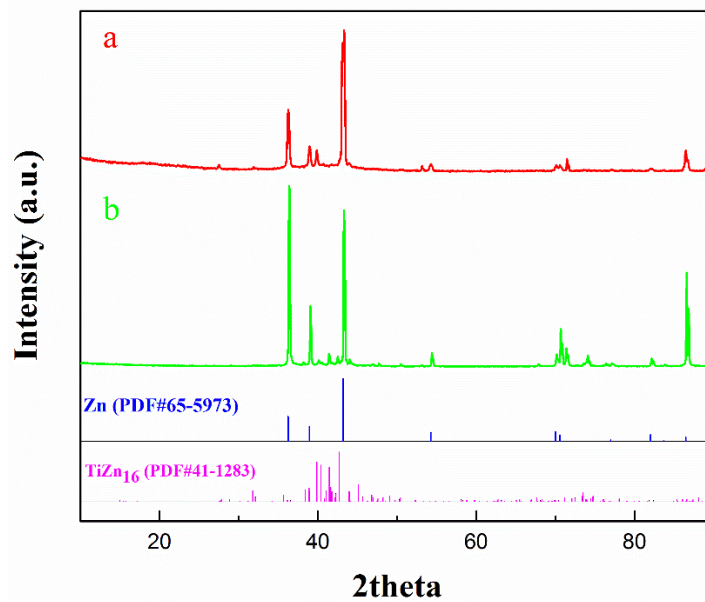
Figure 4. XRD patterns of Zn/TiO_2 electrode after potentiostatic electrolysis at -1.5 V for 2 h, (a) Micro-diffraction (b) Ordinary diffraction

In addition to pure metallic zinc and a small amount of titanium-zinc $TiZn_{16}$ alloy phase, there was no oxides of titanium and zinc. Thermodynamic calculation suggested that the Gibbs free energy for the oxidization reaction of titanium and zinc in air at room temperature is negative, natural oxidation of the product is possible. For comparison, the same pre-melting and pre-electrolysis processes were carried out. The images of SEM and mapping display in fig 5. The dark regions in Zn matrix were the zones of titanium enrichment after potentiostatic electrolysis at -1.5 V for 2 h. The results of the mapping in the control group indicated that there was no rich-titanium region in the monitoring area and little Ti distributed as scattered dots. It means that liquid Zn can't reduce TiO_2 powder and this viewpoint was supported by thermodynamic calculation.

The reaction of electroreduction of TiO_2 in molten $CaCl_2$ was proposed and studied [7]. There are three steps which should occur towards the electroreduction reaction of TiO_2 [26]: Firstly, mass transfer of oxygen from the bulk of the oxide toward the electrode surface. Secondly, charge transfer at the interface between the cathode and the electrolyte melt. Finally, pore diffusion of O^{2-} dissolved in the melt through the pores of the solid cathode. In this electrolysis process, Zn/TiO_2 is used as the cathode. It is found that TiO_2 is reduced to Ti after two hours electrolysis. Some researchers indicated TiO_2 was reduced by means of an electrochemical process, and the reduction was conducted in several steps [27-29]. In this study, TiO was found in the sample. Wang [30] indicated that there is a two-step process for the reduction reaction of TiO_2. TiO_2 is reduced to the intermediate product TiO, and then reduced to pure Ti. The liquid Zn metal formed the alloys with titanium on the surface of zinc matrix. ZnO was also found because of zinc combined with oxygen ion in the melt.
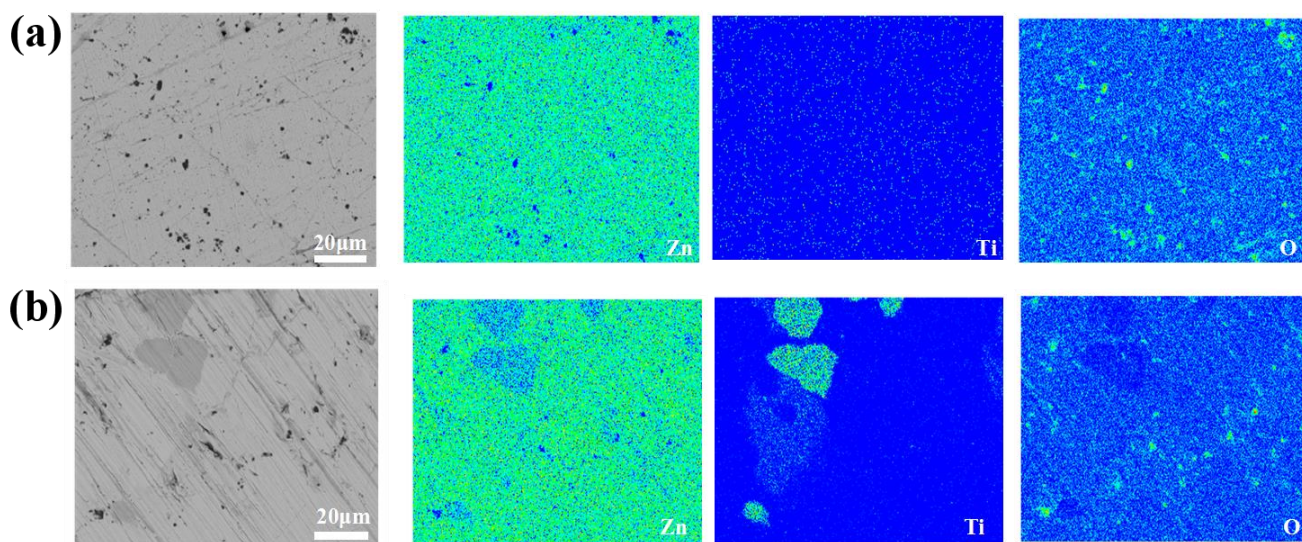
Figure 5. Images of SEM and EDS mapping (a) Heat preservation for 2h (b) Potentiostatic electrolysis at -1.5 V for 2 h

3.3 Rich titanium slag compound electrode electrolysis

It can be seen from table 1 that the chemical composition of the rich titanium slag is complex. The content of TiO_2 reaches 70 wt%. In order to clarify the possible decomposition sequence of the

oxide in rich titanium slag, the decomposition potentials were calculated in the table 3. It is suggested that Ti was deposited before Al, Mg, Ca which has a thermodynamics reducing effect on TiO_2. The electrolysis of voltage was raised to -2.8 V.

Table 3. The Standard Gibbs free energy ΔG^0 and decomposition potentials ΔE^0 for different reactions at 1123K

Reaction	$\Delta G^0/kJ \cdot mol^{-1}$	$\Delta E^0/$ V vs. (O_2/O^{2-})
$TiO_2=Ti+O_2(g)$	740.993	-1.92
$2/3Fe_2O_3 = 4/3Fe + O_2(g)$	352.484	-0.91
$SiO_2=Si+O_2$	708.915	-1.83
$2MgO=2Mg+O_2$	958.545	-2.48
$2/3Al_2O_3=4/3Al+O2(g)$	880.087	-2.28
$2CaO=2Ca+O2$	1034.800	-2.68
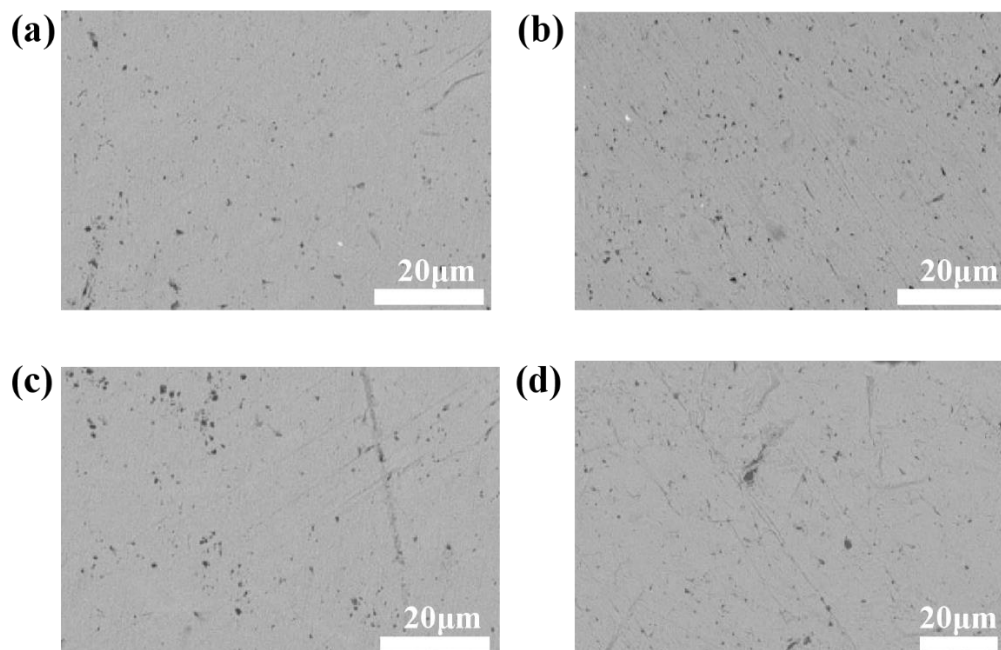
Figure 6. The SEM images of production after electrolysis without pre-melting, (a) Rich titanium slag with Zn electrode potentiostatic electrolysis at -2.8 V for 2h (b) Rich titanium slag with Zn electrode potentiostatic at -2.8 V for 5h (c) TiO_2/Zn electrode potentiostatic electrolysis at -1.6 V for 3 h (d) TiO_2/Zn electrode potentiostatic electrolysis at -1.8 V for 3 h
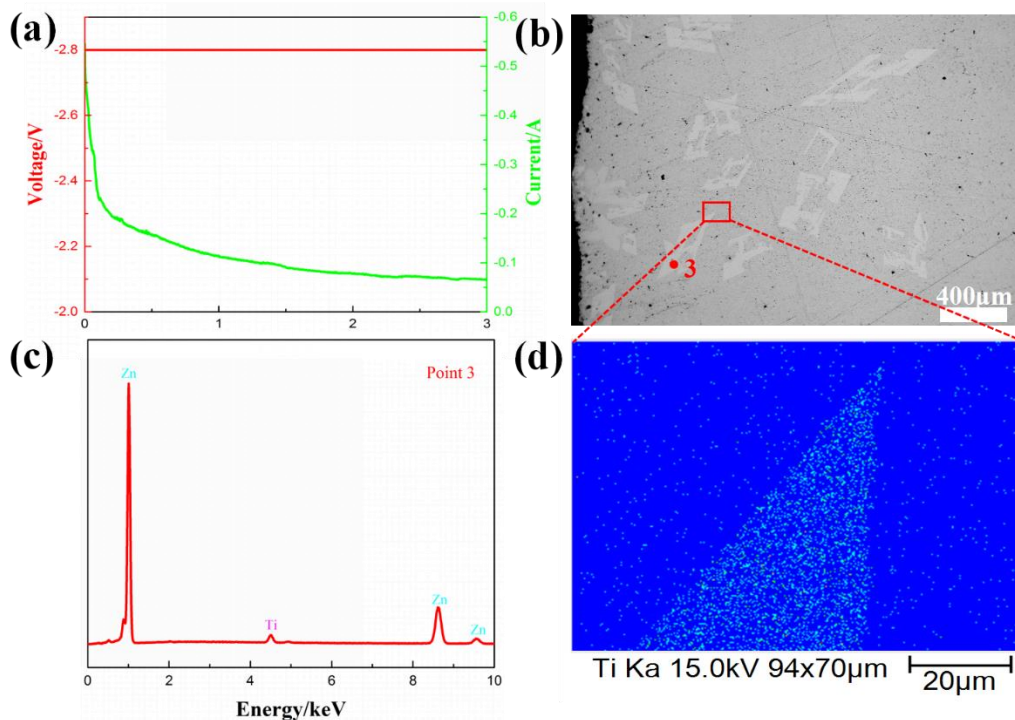
Figure 7. (a) Current-time curves (b) Images of SEM (c) EDS point scan (d) Mapping of high titanium slag on Zn electrode potentiostatic electrolysis at -2.8V for 3 h

The influence of the pre-melting and the electrolysis time were investigated. There was no metal Ti precipitated in Zn matrix when electrochemical experiment without pre-melting process. Carbon was observed in matrix and increased along with electrolysis time. The same situation was occurred in the electrolysis of TiO_2/Zn electrode even if elevated the voltage and electrolysis time. Figure 6 reveals the truth that only holes and scratches emerged in the matrix. The reason might be that zinc didn't melt so that there was a bad connection between zinc matrix and TiO_2. The pre-melting before the electrolysis is beneficial for increasing contact area when the metal completely melted. Liquid zinc can be wetting TiO_2, and then the reaction rate would be faster.

The pre-melting time was restored to 1 h. The potentiostatic electrolysis of rich titanium with Zn electrode for 3h was carried out and shown in fig 7. The current decreased overall. Lots of brighter area appear again where the content of titanium was about 5.5 at% analyzed by EDS. Subsequently, another test was done and the electrolysis time extended to 6 h. The current dropped to 30mA in 1h as shown in fig 8(a). A line-type area with same molecular ratio of Ti was detected. Comparing fig 6 with fig 5, 7 and 8, it is indicated that the reduction of Ti was occurred in the electrolysis of TiO_2 or rich titanium slag with Zn electrode while the pre-melting process was carried out. The later prolongation of electrolysis time has no effects on the percentage of Ti, as we can see that the current mainly gets steady in 1 h.
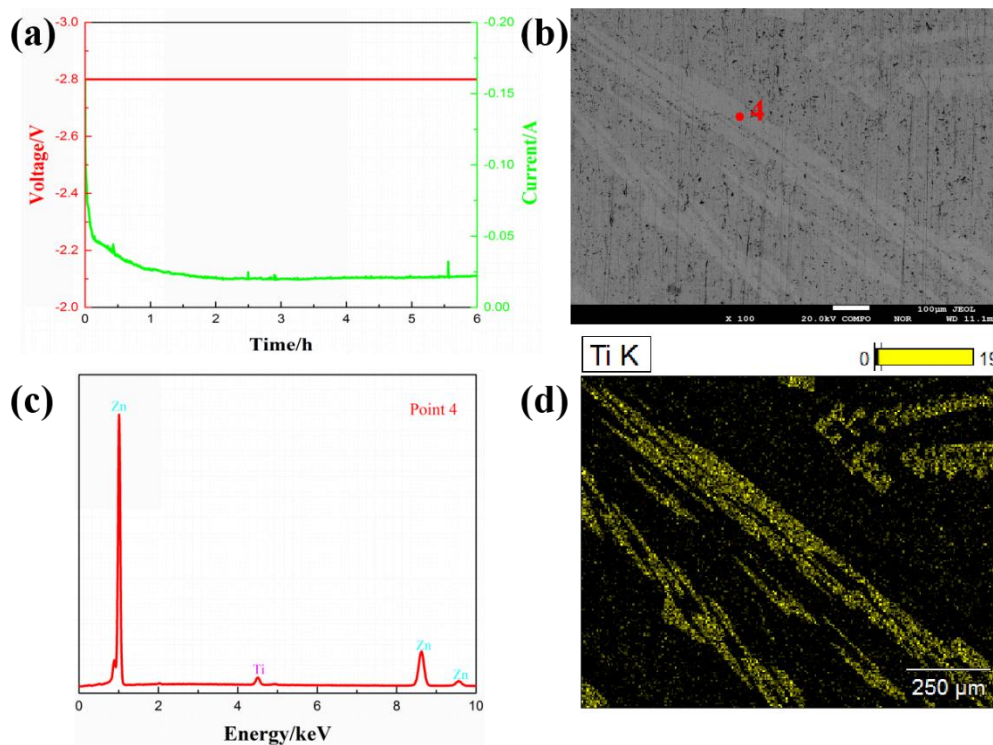
Figure 8. (a) Current-time curves (b) Images of SEM (c) EDS point scan (d) Mapping of high titanium slag on Zn electrode potentiostatic electrolysis at -2.8V for 6 h

Current decreased sharply in short time as shown in fig 9(a) when the pre-melting time extended to 3 h and the electrolysis time was 3 h. The content of Ti in the different enrichment region reached 24.3 at%, 5.8 at%, respectively. Simultaneously, metal element in the rich titanium slag were also discovered. Al appeared in the region where the proportion of titanium was high. Calcium was detected as lump-type in matrix without Ti. Mg and Si distributed scattered. In other words, the oxides of metal in rich titanium slag was reduced and this method was suit for the smelt of metal such as Si and Mg. Figure 10 shows the result of line scan, it indicated that the content of metal in rich region followed the result of point scan. The compositions of production confirmed were shown in table 4 by EDS point scan. The sample analyzed by XRD was shown in fig 11.

Although calcium was detected and some researchers considered that the reduction is a calciothermic reduction process [31, 32], Wang [33] found that TiO_2 pellets can be electrochemical reduced step by step without Ca metal. Qiu [34] discussed that the electro-reduction process is dominated by direct electron transfer to the metal oxide. The Ca metal plays the simple role of an electron donor, even in the presence of a large amount of formed Ca. It was also found that SiO_2 can be electrochemically reduced to form liquid Si–Zn alloy, where Si particles were precipitated on the upper of zinc matrix during cooling process because they floated and aggregated in the liquid phase owing to their lower density [19].

The electro-deoxidation of any oxide pellet starts at the metal/oxide/electrolyte three phase interlines [10]. The advantages when the liquid metal is used as the cathode has been discussed in the previous study paper [35]. The interface area between liquid zinc and TiO_2 increases dramatically

compared to the oxide pellet wound by the metal wire. It is beneficial to increase the interface and the reaction rate.
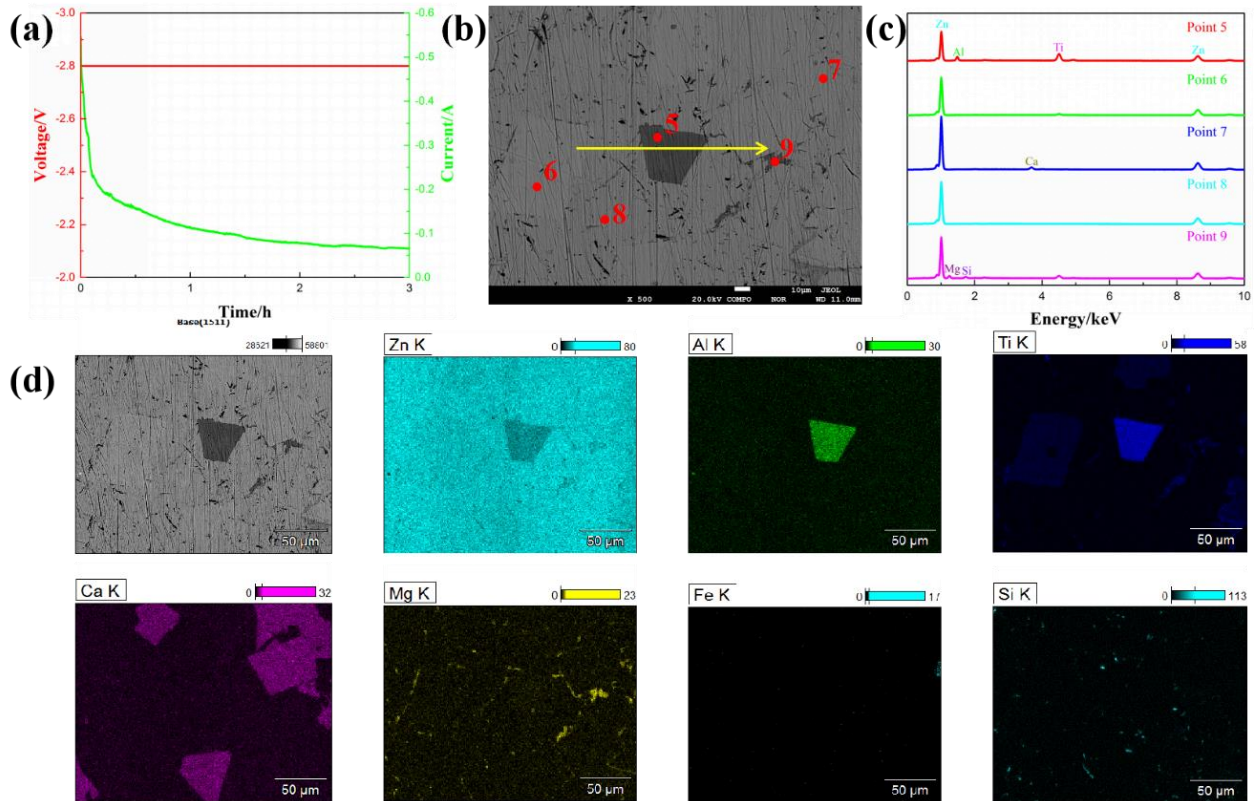
Figure 9. (a) Current-time curves (b) Images of SEM (c) EDS point scan (d) Mapping of high titanium slag on Zn electrode potentiostatic electrolysis at -2.8V for 3 h
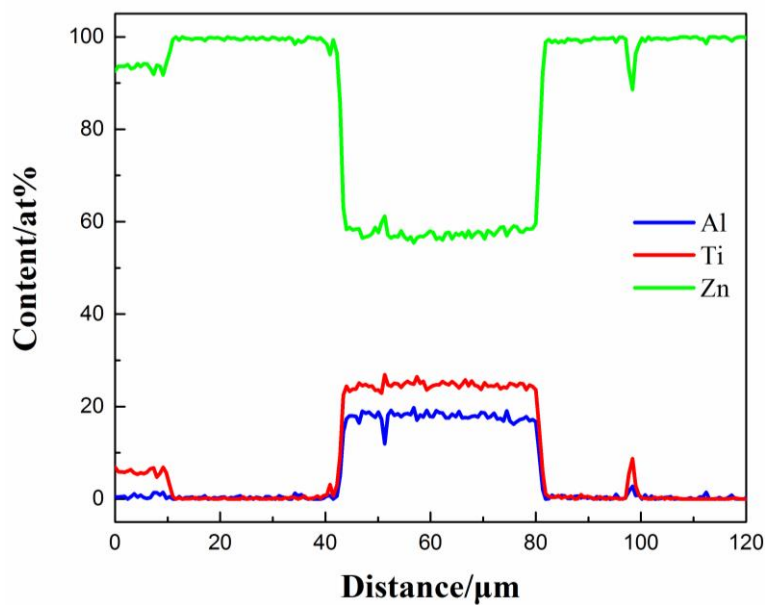
Figure 10. EDS line scan of rich titanium slag on Zn electrode potentiostatic electrolysis at -2.8V for 3h
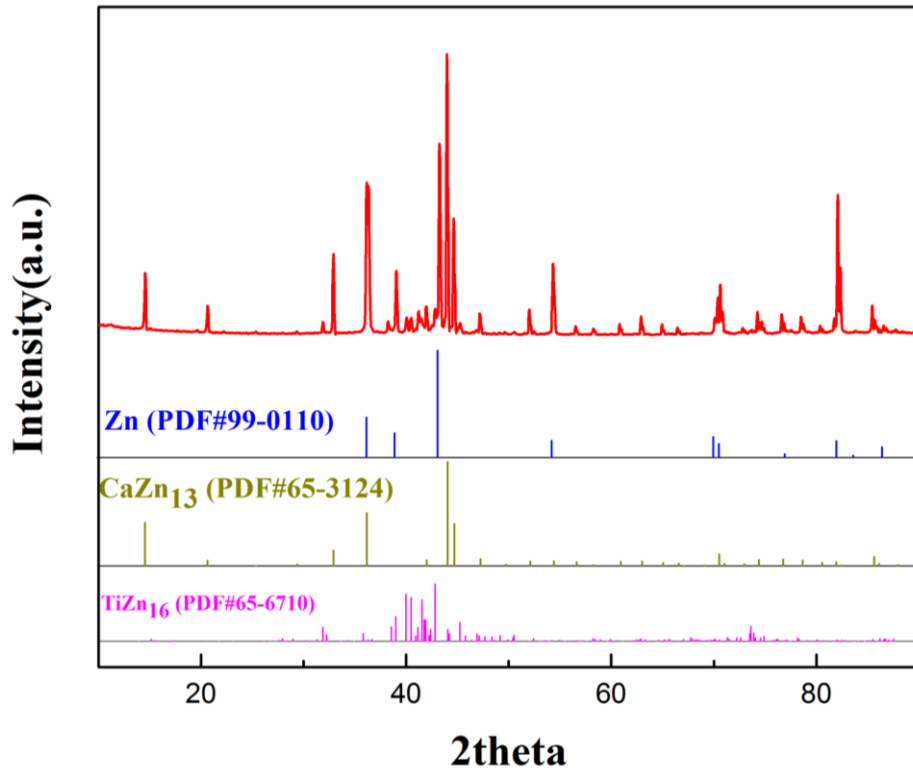
Figure 11. XRD patterns of rich titanium slag on Zn electrode potentiostatic electrolysis at -2.8V for 3 h
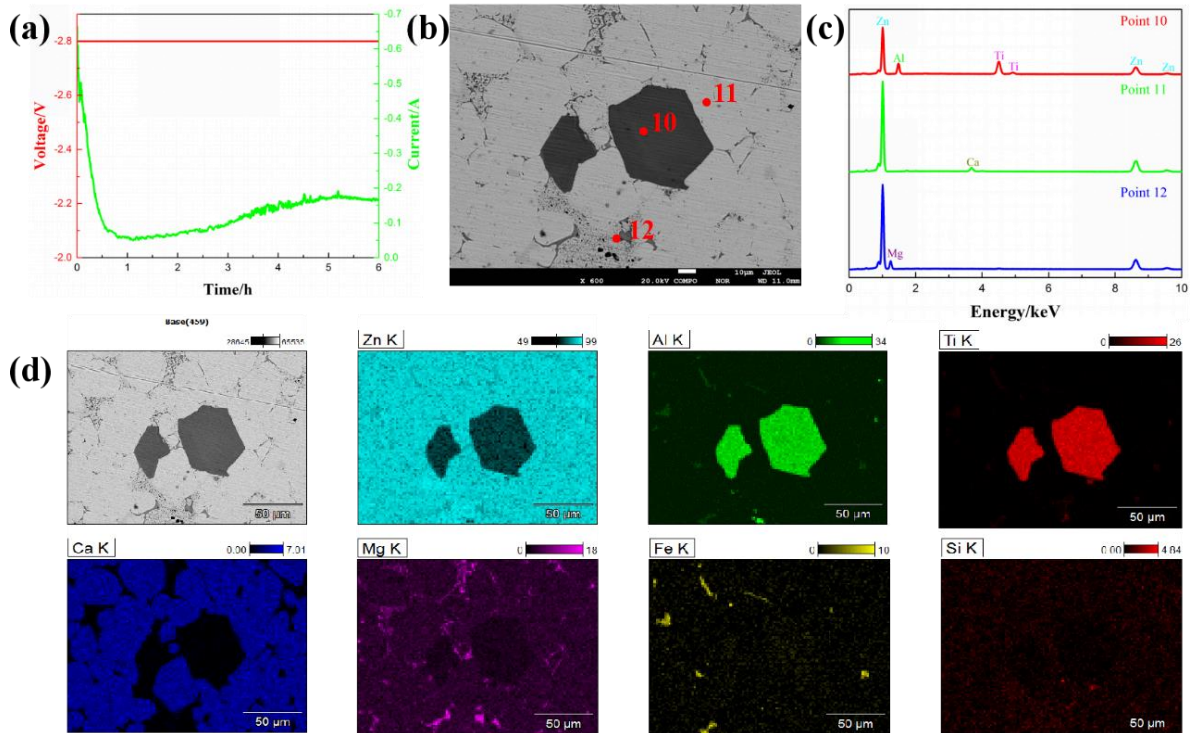
Figure 12. (a) Current-time curves (b) Images of SEM (c) EDS point scan (d) Mapping of rich titanium slag with Zn electrode potentiostatic electrolysis at -2.8V for 6 h

Table 4. The compositions of production confirmed by EDS point scan

Exp.	Feed	Pre-melting /h	Voltage /V	Electrolysis /h	No.	Contents of element in EDS point scan
1#	TiO_2	3	-1.5	2	1	Zn 58.7 at%, Ti 26.3 at%, Al 15 at%
	TiO_2	3	-	-	2	Zn 100 at%
2#	Slag	1	-2.8	3	3	Zn 84.8 at%, Ti 5.5 at%, C 9.6 at%
3#	Slag	1	-2.8	6	4	Zn 91 at%,Ti 5.5 at%, C 3.5 at%
4#	Slag	3	-2.8	3	5	Zn 57.3 at%,Ti 24.3 at%, Al 18.4 at%
	Slag	3	-2.8	3	6	Zn 94.2 at%, Ti 5.8 at%
	Slag	3	-2.8	3	7	Zn 92.2 at%, Ca 7.8 at%
	Slag	3	-2.8	3	8	Zn 100 at%
	Slag	3	-2.8	3	9	Zn 65.1 at%,Ti 9.9 at%, Mg 18.6 at%, Si 6.4 at%
5#	Slag	3	-2.8	6	10	Zn 48.4 at%, Ti 25.4 at%, Al 26.3 at%
	Slag	3	-2.8	6	11	Zn 91.1 at%, Ca 7.0 at%, Si 1.9 at%
	Slag	3	-2.8	6	12	Zn 65.5 at%, Ti 0.8 at%,Mg 33.7 at%

There was $TiZn_{16}$ alloy and calcium-zinc $CaZn_{13}$ alloy. Figure 12 illustrates the results when the electrolysis time was extended to 6 h. Ca diffused in the Zn matrix, the content of Al was increased. The region with low-scale Ti disappeared. Ti and Al enriched in the dark polygon area, where the content reached 25.3 at%,26.3 at%, respectively. Fe, Si, Mg were asymmetrically distributed in Zn matrix. The increasing of electrolysis time was no influences of Ti instead of raising the ration of Al, Ca.

4. CONCLUSIONS

The electrochemical redox processes of In_2O_3 was studied using a liquid indium working electrode at 450 °C in molten LiCl-KCl. Two reduction peaks were observed in the cathodic scan for In_2O_3. Reduction of In_2O_3 occurs at -1.0 V. Another peak is considered to be the reduction of molybdenum oxide. Liquid tin and zinc metals were used as cathode taking into account increasing the contacting area. Constant voltage electrolysis was performed at 1.7 V for 2h. The reduction reaction occurred at the interface of the oxide pellets and the cathode. Sn-In alloys were detected after the electrolysis of In_2O_3 and ITO with the tin cathode. The result showed that indium can be produced at a liquid cathode. ITO was reduced strongly when liquid zinc was used as the cathode. Based on the feasibility experiments, further work is required for improving the kinetics of the reaction and measuring the current efficiency.

An effective way to extract Ti from rich titanium slag with Zn electrode by molten salt has been investigated. The electrochemical behaviors of Zn electrode and TiO_2/Zn electrode in molten $CaCl_2$ were investigated. The depolarization of Zn electrode was confirmed by comparing the deposition position of Ca in different electrode. The reduction of TiO_2 was performed at potential range from -0.77 V to -1.73 V vs. Ag/AgCl. After potentiostatic electrolysis of Zn/TiO_2 electrode, TiO_2 was reduced and enriched in Zn matrix as the phase of $TiZn_{16}$, the content of Ti reached 26.3 at% in enrichment area. The pre-melting was the key process for the enrichment area of titanium in the product. As the pre-melting carried out, Fe, Si, Al, Mg, Ca were observed in Zn matrix after electrolysis. Al appeared in the zones with high content of Ti. Ca deposited in the area without Ti and spread to the all matrix while the electrolysis of time was extended. Fe, Mg, Si irregularly scattered in the detected area. When the pre-melting time in the electrolysis of rich titanium slag was extended from 1h to 3h, the content of Ti in rich region was raised from 5.5 at% to 25.3 at%. The later extension of electrolysis time (after 1h) has no influences of the content of titanium.

References

1. H. Attar, S. Ehtemam-Haghighi, D. Kent, M.S. Dargusch, *Int. J. Mach. Tool. Manu.,* 133 (2018) 85.
2. X. Liu, P. K. Chu, C. Ding, *Mat. Sci. Eng. R.*, 47 (2004) 49.
3. W. Kroll, *E. Electrochem. Soc.,* 78 (1940) 35.
4. G. Crowley, *Adv. Mater. Process.*, 161 (2003) 25.
5. J. Li, Z.T. Zhang, X.D. Wang, *Ironmak Steelmak.*, 39 (2012) 414.
6. W. Weng, M. Wang, X. Gong, Z. Wang, D. Wang, Z. Guo, *J. Electrochem. Soc.,* 164 (2017) D551.
7. G.Z. Chen, D.J. Fray, T.W. Farthing, *Nature*, 407 (2000) 361.
8. K. Yasuda, T. Nohira, K. Kobayashi, N. Kani, T. Tsuda, R. Hagiwara, *Energy Technol – Ger.*, 1 (2013) 245.
9. K. Yasuda, T. Nohira, K. Amezawa, Y.H. Ogata, Y. Ito, *J. Electrochem. Soc.,* 152 (2005) D69.
10. G.Z. Chen, E. Gordo, D.J. Fray, *Metall. Mater. Trans. B.*, 35 (2004) 223.
11. E. Gordo, G.Z. Chen, D.J. Fray, *Electrochim. Acta*, 49 (2004) 2195.
12. S. Jiao, D.J. Fray, *Metall. Mater. Trans. B.*, 41 (2010) 74.
13. S. Bossuyt, S.V. Madge, G.Z. Chen, A. Castellero, A.L. Greer, *Metall. Mater. Trans. A.,* 375 (2004) 240.
14. K.S. Mohandas, D.J. Fray, *Metall. Mater. Trans. B.,* 40 (2009) 685.
15. C. Wu, M. Tan, G. Ye, D.J. Fray, X. Jin, *ACS. Sustain. Chem. Eng.*, 7 (2019) 8340.
16. Y. Kado, A. Kishimoto, T. Uda, *J. Electrochem. Soc.*, 160 (2013) E139.
17. B. Qin, P. Cui, A.M. Martinéz, E.R. Aune, G.M. Haarberg, *ECS Transactions,* 64 (2014) 249.
18. T. Nohira, A. Ido, T. Shimao, X. Yang, K. Yasuda, R. Hagiwara, T. Homma, *ECS Transactions,* 75 (2016) 17.
19. K. Yasuda, T. Shimao, R. Hagiwara, T. Homma, T. Nohira, *J. Electrochem. Soc.*, 164 (2017) H5049.
20. Y. Ma, A. Ido, K. Yasuda, R. Hagiwara, T. Homma, T. Nohira, *J. Electrochem. Soc.,* 166 (2019) D162.
21. H. Jiao, D. Tian, S. Wang, J. Zhu, S. Jiao, *J. Electrochem. Soc.*, 164 (2017) D511.

22. K.Yasuda, T. Nohira, R. Hagiwara, Y.H. Ogata, *J. Electrochem. Soc.,* 154 (2007) E95.
23. S. Jiao, D.J. Fray, *Metall. Mater. Trans. B.,* 41 (2010) 74.
24. K. M. Axler G. L. Depoorter, *Mater. Sci. Forum.,* 73 (1991) 9.
25. D. A. Wenz, I. Johnson, R. D. Wolson, *J. Chem. Eng. Data,* 14 (1969) 252.
26. X.Y. Yan, D.J. Fray, *Metall. Mater. Trans. B.*, 33 (2002) 685.
27. C. Schwandt, D. J. Fray, *Electrochim. Acta*, 51 (2005) 66.
28. D. T. L. Alexander, C. Schwandt, D. J. Fray, *Acta. Mater.,* 54 (2006) 2933.
29. K. Dring, R. Dashwood, D. Inman, *J. Electrochem. Soc.*, 152 (2005) E104.
30. S. L. Wang, Y. J. Li, *J. Electroanal. Chem.,* 571 (2004) 37.
31. R. O. Suzuki, M. Aizawa, K. Ono, *J. Alloy. Compd.,* 288 (1999) 173.
32. I. I. Park, T. Abiko, T. H. Okabe, *J. Phys. Chem. Solids.,* 66 (2005) 410.
33. B. Wang, K. R. Liu, J. S. Chen, T. Nonferr. Metal. Soc., 21 (2011) 2327.
34. G. Qiu, K. Jiang, M. Ma, D. H. Wang, X. B. Jin, G. Z. Chen, Z. *Naturforsch. A.*, 62 (2007) 292.
35. P. Cui, B. Qin, A. M. Martinez, G. M. Haarberg, *Int. J. Electrochem. Sci.,* 15 (2020) 424.